

Energy band associated with dangling bonds in silicon

S. Mantovani, U. del Pennino, and S. Valeri

Istituto di Fisica dell'Università di Modena, Via Campi, 213/A-41100 Modena, Italy

(Received 20 November 1979)

High-frequency capacitance measurements as a function of applied bias have been performed between 77 K and 250 K on Schottky Pd₂Si-Si diodes, obtained from previously deformed *n*-silicon slices. Having used low dislocation densities and high-resistivity silicon we were able to check, in the range of temperatures investigated, the validity of the half-filled-band model, which assumes the existence of dangling bonds associated with edge-type dislocation. Good agreement between theory and experiments was found, confirming that, with the edge dislocation in silicon, it can be associated with a one-dimensional energy band, of width 0.24 eV and a neutral level E_0 at 0.40 eV above the top of the valence band; it was also confirmed that the edge dislocations are surrounded by cylindrical charge clouds, whose effective radius is comparable with the Debye screening length.

I. INTRODUCTION

In the model of the half-filled band (HFB),¹ it is assumed that in the edge dislocation core there exist dangling bonds which originate a one-dimensional energy band in the semiconductor forbidden gap, with the Fermi level always inside this band. This model has been successfully adopted to interpret experimental results on the electrical effects of dislocations in semiconductors.¹⁻¹⁴ However, some other results,¹⁵⁻¹⁹ sometimes obtained in experimental conditions in which the HFB model could not be properly applied,^{13,20} are in disagreement with the previous ones, mainly concerning the dislocation energy levels. Moreover, recent investigations using weak-beam electron microscopy²¹⁻²³ have shown that dislocations dissociated for most of their length in partial dislocations, and this fact could render the dislocations electrically inactive by a coupling of dangling bonds.^{24,25} There is, therefore, the need of further experimental tests on the existence of the dangling bonds. This can be done, for example, by electrical measurements, using a technique able to discriminate between the effects expected from a row of dangling bonds (having a many-electron character) and those due to other possible electrically active centers (such as point defects, impurities, and defect aggregates activated or redistributed in the sample during the plastic deformation). To this end we employed a technique which had already been found to be very suitable,^{6,14} consisting in high-frequency measurements at different temperatures of the capacitance-voltage (C-V) characteristics of Schottky diodes made of previously deformed semiconductors.

In the present work we extended some preliminary investigations on Au-*n* silicon Schottky

diodes¹² mainly using palladium silicide-silicon-Schottky diodes, which give more stable and reliable characteristics,²⁶ and can be obtained by annealing at relatively low temperatures (~570 K) for short times (~30 min).²⁷ To be in the validity range of the HFB model, we operated with high-resistivity silicon, low-dislocation densities, and not too low temperatures.¹³

II. EXPERIMENTAL

Starting material was monocrystalline *n*-silicon, doped with P, with a resistivity of 500 Ω cm, in form of {111} slices, with a thickness ranging between 200 and 300 μm, and initial dislocation density of about 10³ cm⁻². The slices were deformed, for a few minutes at 1023 K, by bending with different radii around the ⟨112⟩ direction and flattening, in a vacuum better than 10⁻⁶ torr. The subsequent cooling rate was lower than 5 K/min. The deformation temperature was selected to enhance the direct effect of the dislocations, as higher temperatures seem to produce agglomerates of point defects and impurities,¹⁶ while lower temperatures can lead to the formation of stable aggregates of point defects along the slip planes.²⁸ The total dislocation densities introduced were in the range (0.5-5) × 10⁶ cm⁻², of which, as concluded from transmission electron microscope observations, 80% were inclined with respect to the (111) plane and could be approximately counted by etching, and about 20% were lying in the plane; about 75% of the total were of the edge type. Such dislocation densities are sufficiently low to avoid large errors in the etch-pits countings.

The Schottky diodes were obtained by the growth of a 500-Å-thick palladium silicide film on the silicon deformed slices by a technique already de-

scribed²⁹; the back contact was obtained afterward by evaporated aluminum. The Pd₂Si-film area was circular, with a radius of 6 mm; its presence and homogeneity was checked by 2-MeV ⁴He⁺ back-scattering spectrometry and x-ray diffractometry.

The capacitance measuring apparatus, based on a lock-in amplifier, has been described elsewhere.⁶ The rate of cooling the diodes to the liquid-nitrogen temperature did not exceed 1 K/min. After the capacitance measurements, the diodes were etched to count the etch pits by an optical microscope; the counting was made on 10 zones of the diode area and only those samples with a homogeneity of better than 10% were considered.

III. RESULTS AND DISCUSSION

A. High reverse voltages

The diode capacitance C , as a function of the applied bias V , was measured reverse-biasing the diode from 0 V in a few seconds. As at temperatures below 250 K, the time constant for the thermal emission of trapped carriers is quite long, their concentration during the measurement keeps constant and equal to its equilibrium value ($V=0$); therefore it is possible to obtain, at the different temperatures, the effective donor-concentration profile at equilibrium, $N_D(x)$, from the expression valid for Schottky diodes:

$$N_D(x) = -\frac{C^3}{A^2 q \epsilon} \left(\frac{dV}{dC} \right), \quad (1)$$

where ϵ is the silicon permittivity, q the electronic charge, A the diode area, and x the depletion-region width, given by $x = \epsilon A / C$.

In our samples at reverse biases higher than 10 V, the equilibrium-concentration profiles come out to be constant at each temperature. In Fig. 1 we report, as a function of the temperature, these concentrations for three deformed samples and for a reference one, which had been subjected to the same heat treatment except for the deformation.

From the profile curves it is possible to obtain two quantities. The first one is the dislocation occupation function $f = (N_D - N'_D) / N_s$, where N'_D and N_D are the effective donor concentrations in the deformed sample and in the reference one (where it was equal to that in the virgin sample), and N_s is the dangling bond concentration; N_s is given by N_\perp / a , with N_\perp the total edge-dislocation density, deduced from etch-pit countings, and a the distance between dangling bonds, for which we took the average value of 3.67 Å. [In our samples, $\frac{1}{3}$ of the edge dislocations were of the 90° type

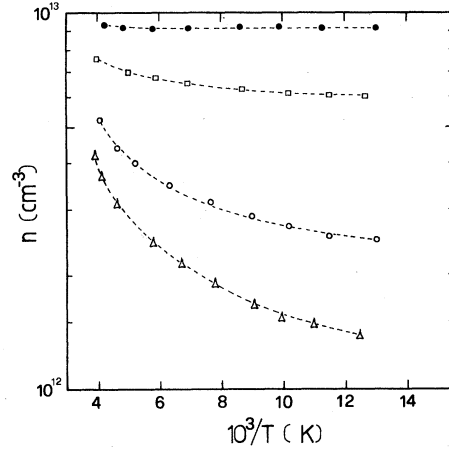


FIG. 1. Effective carrier concentration as a function of the reciprocal temperature, as calculated from C-V measurements. (●): reference sample; (□): B1; (○): B2; (△): B3. Edge-dislocation density of the bent samples N_\perp : B1: $7.5 \times 10^5 \text{ cm}^{-2}$; B2: $1.8 \times 10^6 \text{ cm}^{-2}$; B3: $2.4 \times 10^6 \text{ cm}^{-2}$.

($a = 3.32 \text{ \AA}$) and $\frac{2}{3}$ were of the 60° type ($a = 3.84 \text{ \AA}$).] The second quantity obtained from the profile curves is the value of the Fermi level, measured from the top of the valence band far from the dislocation, E_F , by means of

$$E_F = E_G - kT \ln(C_c T^{3/2} / N'_D). \quad (2)$$

E_G is the silicon band-gap width (whose temperature dependence must be accounted for³⁰) and C_c is $5.4 \times 10^{15} \text{ cm}^{-3} \text{ K}^{-3/2}$. The experimental values of E_F as a function of f are indicated by symbols in Fig. 2.

In the HFB model the value of the Fermi level is related to the highest-occupied level in the dislocation energy band when the dislocation is neu-

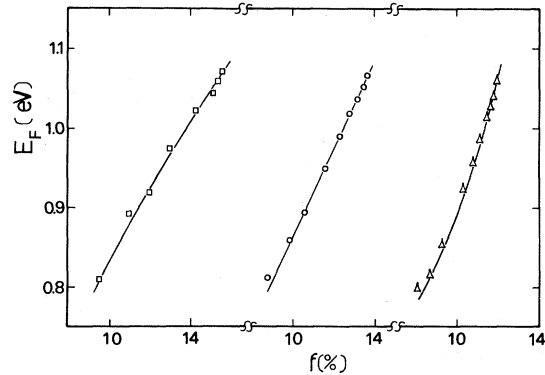


FIG. 2. Fermi level versus the edge-dislocation occupation function f . Experimental values for B1 (□), B2 (○), and B3 (△). The solid lines are calculated according to Eq. (3) with $E_0 = 0.40 \text{ eV}$.

tral, measured from the top of the valence band, E_0 , by

$$E_F = E_0 + \left(\frac{q^2 f}{2\pi\epsilon a} \right) \left[\ln \left(\frac{\lambda_D f}{a} \right) + \frac{1}{4} \left(\frac{N_D}{N_D'} + 1 \right) \right], \quad (3)$$

where $\lambda_D = (\epsilon kT/q^2 N_D')^{1/2}$ is the Debye screening length. The solid lines in Fig. 2 represent the best fits of E_F as a function of f , calculated by use of Eq. (3) assuming $E_0 = 0.4$ eV; the fit is quite good and is in agreement with some preliminary results obtained with Au-Si diodes.¹²

We further note that sample B2 gives the same results as sample BS of Ref. 12, an Au-Si diode from which B2 was obtained after chemical removal of Au and Al, cleaning, and Pd₂Si formation. This confirms that the formation of the Pd₂Si film does not change the electrical characteristics of the starting deformed material.

B. Deep-level analysis

The experimental technique employed to investigate the presence of deep impurity levels,^{31,32} by which some results were already obtained,¹⁴ consists in giving a large reverse bias V_R to a Schottky diode at room temperature, cooling it slowly to about 77 K, and measuring, in a short time, the diode capacitance as the bias is reduced to zero and then increased again to V_R . The large reverse bias given at room temperature and the subsequent cooling cause the space-charge region to be in a steady state, near the liquid-nitrogen temperature. This means that possible deep levels in the upper half of the band gap, located between the interface and where the quasi-Fermi level crosses the deepest level, are not occupied by electrons; as V decreases, the deep levels fill with electrons and keep occupied at their zero-bias thermal-equilibrium concentration during the subsequent biasing. As a consequence, a hysteresis in the C - V curves results, as shown, for example, in Fig. 3 for the sample B1, which is one of the least deformed we investigated. The reference samples do not show, within the experimental errors, such a hysteresis indicating that possible deep levels introduced during the thermal cycles are less than 10^{11} cm⁻³.

The profiles of the net space-charge concentration in the deformed samples, obtained by means of Eq. (1) from the capacitance values measured during the bias decrease, $N_D''(x)$, are shown in Fig. 4, together with the profiles obtained during the subsequent biasing, N_D' . It can be seen that the depolarization profiles are not uniform along the whole depletion region of width L , but only for a length \bar{x} , where they show the same value of the reference samples: $\sim 9.2 \times 10^{12}$ cm⁻³. For $x > \bar{x}$,

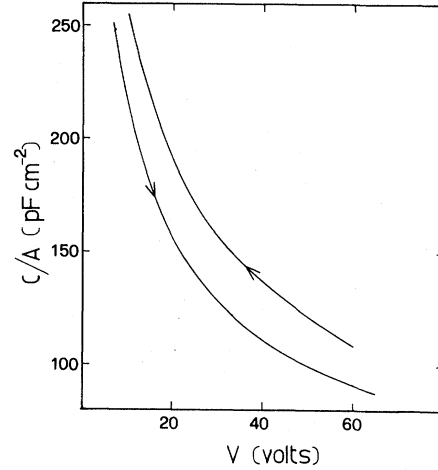


FIG. 3. Capacitance for unit area, C/A , versus reverse bias V , at 79 K for B1; (\leftarrow) during the depolarization after a reverse bias of 60 V at 300 K, (\rightarrow) during the successive biasing.

the concentrations decrease as far as $x = L$ where they reach the thermal equilibrium values of the different dislocation contents. These profiles are not step functions as they would be in the case of discrete deep monolevels, indicating the presence of a dense distribution of levels in the same half-gap as the Fermi level; this is just what is predicted for dislocation by the HFB model.

From the profiles it is possible to calculate at each x , the value of $f(x) = [N_D - N_D''(x)]/N_s$, and of

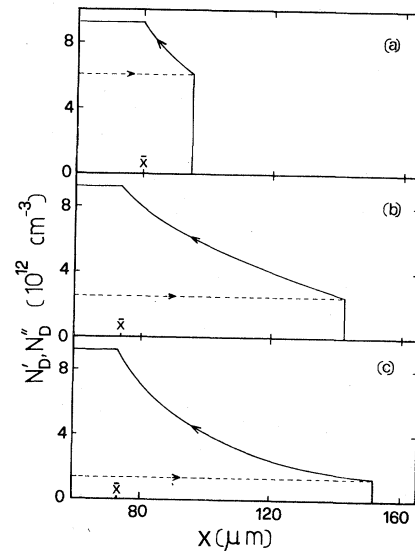


FIG. 4. Net charge concentration in the depletion region. Solid lines correspond to decreasing bias, dashed lines to increasing bias; (a): sample B1 at 79 K (60 V at 300 K); (b): sample B2 at 77 K (95 V at 300 K); (c): sample B3 at 80 K (75 V at 300 K).

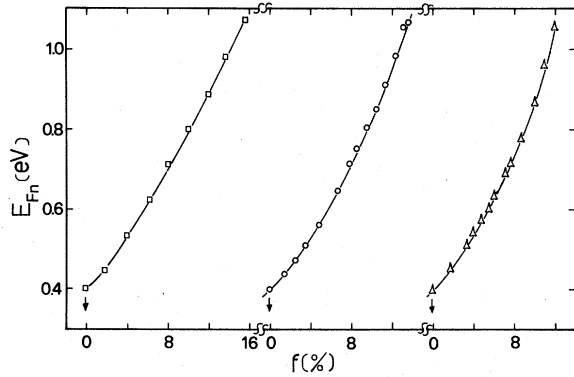


FIG. 5. Quasi-Fermi level E_{Fn} versus the edge-dislocation occupation function f . Experimental values: (□) B1, (○) B2, (△) B3. Solid lines calculated according to Eq. (3) with $E_0=0.40$ eV and $T=79$ K (B1), 77 K (B2), and 80 K (B3).

the quasi-Fermi level for electrons, computed from the top of the valence band far from the dislocation E_{Fn} , with the assumptions: $E_{Fn}=0.4$ eV at $x=\bar{x}$ [where $f(x)=0$], $E_{Fn}=E_F$ at $x=L$, and E_{Fn} proportional to the electrostatic potential between \bar{x} and L .

On the other hand, if we suppose Eq. (3) to be valid also in the space-charge region (with the replacement of E_F with E_{Fn}), we can calculate the values of E_{Fn} for different values of f , taking $E_0=0.4$ eV and T as the temperature of measurement. The values so obtained can be compared with those found experimentally, as shown in Fig. 5.

It can also be useful to show as a function of the

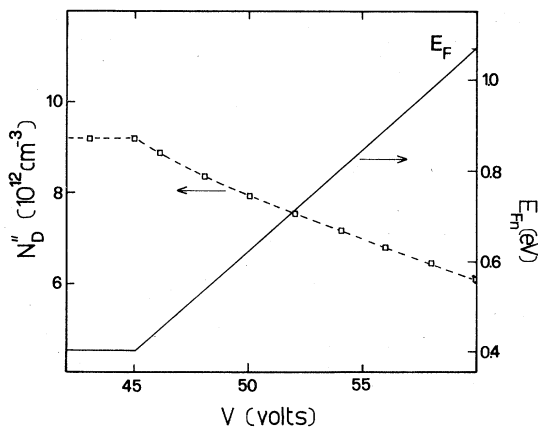


FIG. 6. Net charge concentration for sample B1 as a function of the potential along the space-charge region, measured at 79 K decreasing the reverse bias of 60 V given at 300 K; (□): experimental values as derived from C - V measurements, dashed lines as derived from Eq. (3) with $E_0=0.40$ eV, and E_{Fn} values as shown by the solid line.

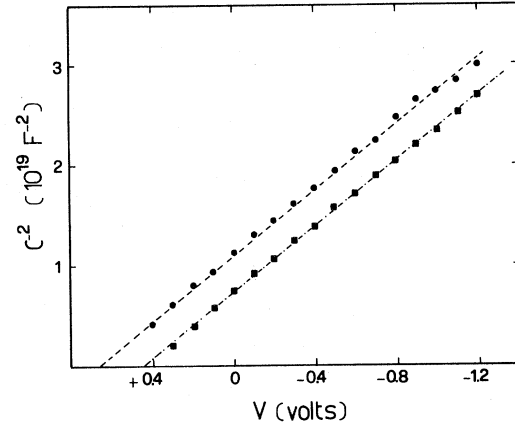


FIG. 7. Typical C^{-2} versus V plots for a Pd_2Si -Si Schottky reference diode at 77 K (●) and 207 K (■).

potential along the space-charge region both the charge concentration obtained from the C - V measurements at decreasing bias and that calculated by use of Eq. (3) with the aforesaid assumptions. This is done in Fig. 6 for sample B1. The agreement between experimental results and model predictions are quite good, confirming also the validity of the assumptions made.

C. Low reverse voltages

The values of C^{-2} as a function of the applied bias V , are reported in Fig. 7 for a reference sample at the temperatures of 207 and 77 K; the barrier potential V_B can be calculated from the intercept V_I of the C^{-2} straight line with the V axis, according to the expression

$$V_B = V_I + kT/q + V_F, \quad (4)$$

where $V_F = (E_G - E_F)/q$.

In this case, V_B results to be (0.74 ± 0.02) eV, as already found for the Pd_2Si barrier.³³ Figure 8 presents a typical example of the behavior of C^{-2} vs V for a deformed sample (B2) at different temperatures. The curves are very different from those of the reference sample, as they are all bent downwards and the bending increases with decreasing temperature (and increasing edge-dislocation content); they are straight lines in a narrow voltage range before the intersections with the V axis.

The experimental temperature dependence of V_I , with that calculated by (4), taking $V_B=0.75$ V, are shown in Fig. 9 for sample B2. The mean value of V_B obtained from all the deformed samples is (0.74 ± 0.03) V, coinciding with that of the reference samples. We can say, on the basis of these results, that the dislocations do not alter the expected barrier potential.

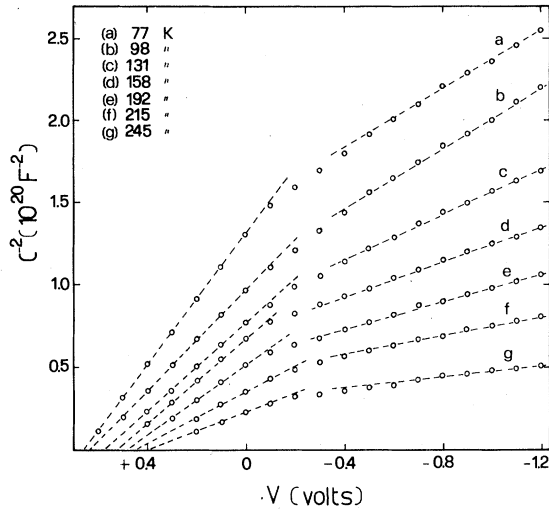


FIG. 8. C^{-2} versus V plots at different temperatures for sample B2: (a) 77 K, (b) 98 K, (c) 131 K, (d) 158 K, (e) 192 K, (f) 215 K, and (g) 245 K.

The bending of the C^{-2} curves can be explained by a geometrical effect³⁴ of reduction of the effective junction area, due to the space-charge cylinders surrounding the edge-type dislocations. This effect, already noted in silicon³⁵ and germanium,¹¹ should derive from the fact that when the depletion layer width is comparable with or smaller than the effective cylinder radius r_1 , the effective area of the plane capacitor given by the junction becomes $A' = (A - A_1)$ where A_1 is the sum of all the cross sections of the space-charge cylinders: $A_1 = N_1 \pi r_1^2$. Accordingly, A' can be obtained from the experimental results at voltages near V_I by $A' = AC'/C$, where the capacitance of the reference sample C and that of the deformed sample C' must be measured at the same V .

From the knowledge of A' , and in the hypothesis

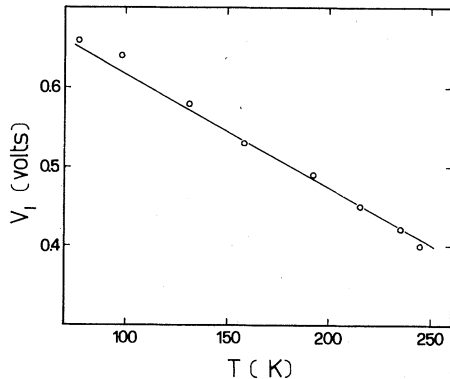


FIG. 9. Intercept voltage V_I of the sample B2 as a function of the temperature: (○) experimental values; solid line calculated from Eq. (4) assuming $V_B = 0.75$ V.

of no dislocation overlap, the effective cylinder radius r_1 can be calculated by

$$r_1 = \left(\frac{A - A'}{N_1 \pi} \right)^{1/2}. \quad (5)$$

The values of r_1 referring to the deformed samples are shown at different temperatures in Fig. 10; for comparison, also plotted as a solid line is the behavior of the Debye screening length λ_D as a function of the temperature, for the three deformed samples already shown. The dot-dashed lines in Fig. 10 represent the temperature dependence of the space-charge cylinder radius according to the Read³⁶ expression

$$r_R = (f/N_D \pi \alpha)^{1/2}, \quad (6)$$

which is obtained in the hypothesis of space-charge cylinders with sharp boundaries. It can be seen that $r_1 \cong \lambda_D < r_R$, and therefore one of the basic assumptions of the HFB model seems confirmed, namely, that the screening clouds around the charged dislocations, mainly due to a rearrangement of free carriers, do not have sharp boundaries but decay exponentially with a characteristic length λ_D . This picture should be no more valid at very low temperatures, where a transition to the Read model is expected; this tendency can be actually recognized in the behavior of the r_1 's of the least deformed samples, which are a little higher than λ_D near 77 K.

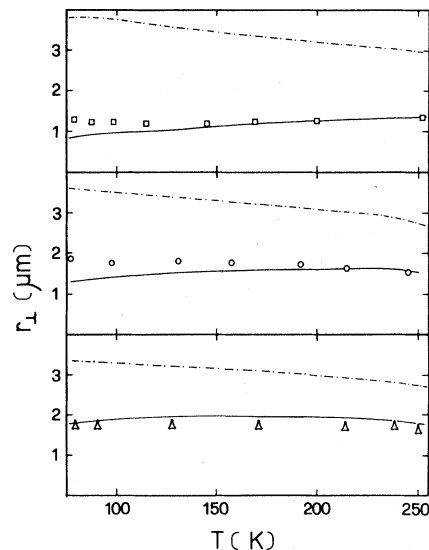


FIG. 10. Experimental effective radius r_1 of the space-charge cylinders surrounding the edge dislocations vs T ; (□) B1, (○) B2, and (△) B3. Solid lines are the calculated Debye screening lengths λ_D and dot-dashed lines are the space-charge cylinder radii according to the Read theory (Ref. 36) r_R .

The HFB model can be properly applied only if the single dislocations can be considered independent of each other, and this is possible if the mean distance between neighboring dislocations is not lower than twice the effective cylinder radius. This condition is fulfilled in the whole temperature range investigated and for the dislocation densities in our samples.

The values of r_1 found are also in good agreement with SEM (scanning electron microscope) observations.^{37,38}

IV. CONCLUSIONS

The HFB model can be used to describe the energy levels associated with edge-type dislocations if the following conditions are fulfilled¹³:

(A) The dislocation can be described as a scattering center, that is, the mean-free path of free carriers is higher than λ_D .

(B) The screening length of the dislocation line charge is mainly due to a free-carrier redistribution; i.e., $(N_D/C_c T^{3/2}) \exp(E_C - E_D)/kT < 1$, where E_C is the bottom of the conduction band and E_D the energy level of the shallow donors.

(C) No consistent overlap occurs among the space-charge cylinders around the dislocations.

In our case, conditions (A) and (B) are fully satisfied in the whole temperature range of measurements, for the high resistivity of the silicon used, and condition (C) is satisfied for the low dislocation densities investigated.

The experimental results obtained for silicon are in substantial agreement with the HFB model, confirming the existence of the dangling bonds, and in particular that:

(1) A half-filled band (with a neutral level E_0

$= 0.40$ eV, in agreement with recent photoconductivity measurements³⁹) is associated to edge dislocations.

(2) The electrical properties of the edge dislocations are similar to those of deep impurities with a dense multilevel spectrum.

(3) The screening of the charge on the dislocations, down to not too low temperatures (77 K) is attained by a rearrangement of free carriers, and the screening clouds decay exponentially with a characteristic length λ_D .

We remind the reader here that previous measurements of reverse diode current³⁵ showed that in silicon the most effective level for the generation-recombination on the dislocation, E_{eff} , is at 0.52 eV above the top of the valence band at dislocation, and coincides with the top of the dislocation band. Therefore, from the knowledge of E_{eff} and of E_0 (0.40 eV) we can give a measure of the width of the dislocation energy band in silicon $2(E_{eff} - E_0) = 0.24$ eV, in good agreement with the results of photoconductivity measurements.³⁹

We note, finally, that our results are also consistent with those obtained by the similar technique of transient capacitance spectroscopy on Schottky barriers,¹⁹ showing that in silicon, besides some energy levels associated with different defect states, there is present a band of "true" dislocation states, centered about 0.35 eV above the top of the valence band and about 0.25 eV wide.

ACKNOWLEDGMENTS

We wish to thank Dr. E. Mazzega for his valuable assistance and Professor A. Loria and Professor G. Ottaviani for their encouragement.

¹W. Schröter and R. Labusch, *Phys. Status Solidi* **36**, 539 (1969).

²H. Weber, W. Schröter, and P. Haasen, *Helv. Phys. Acta* **41**, 1255 (1968).

³W. Schröter, *Phys. Status Solidi* **31**, 177 (1969).

⁴R. Labusch and R. Schettler, *Phys. Status Solidi A* **9**, 455 (1972).

⁵R. Wagner and P. Haasen, *Inst. Phys. Conf. Ser.* **23**, 56 (1975).

⁶S. Mantovani, U. del Pennino, and E. Mazzega, *Phys. Status Solidi A* **35**, 451 (1976).

⁷U. del Pennino and S. Mantovani, *Phys. Status Solidi A* **38**, 109 (1976).

⁸V. A. Grazhulis, V. V. Kveder, V. Yu Mukhina, and Yu. A. Osip'yan, *Zh. Eksp. Teor. Fiz. Pis'ma Red.* **24**, 164 (1976) [*JETP Lett.* **24**, 143 (1976)].

⁹D. Mergel and R. Labusch, *Phys. Status Solidi A* **41**, 433 (1977).

¹⁰D. Mergel and R. Labusch, *Phys. Status Solidi A* **42**,

155 (1977).

¹¹S. Mantovani, U. del Pennino, and E. Mazzega, in *Proceedings of the Vth International Summer School on Defects*, edited by T. Figielski, M. Jastrzebska, and W. Szkielko (Polish Scientific, Warsaw, 1978), p. 225.

¹²S. Mantovani, E. Mazzega, S. Valeri, and U. del Pennino, *Phys. Status Solidi A* **50**, K123 (1978).

¹³W. Schröter, *J. Phys. (Paris) Colloq.* **C6**, 51 (1979).

¹⁴S. Mantovani and E. Mazzega, *J. Phys. (Paris) Colloq.* **C6**, 63 (1979).

¹⁵J. R. Patel, L. R. Testardi, and P. E. Freeland, *Phys. Rev. B* **13**, 3548 (1976).

¹⁶V. A. Grazhulis, V. V. Kveder, and V. Yu Mukhina, *Phys. Status Solidi A* **43**, 407 (1977).

¹⁷V. A. Grazhulis, V. V. Kveder, and V. Yu Mukhina, *Phys. Status Solidi A* **44**, 107 (1977).

¹⁸V. G. Eremenko, V. I. Nikitenko, E. B. Yakimov, and N. A. Yarykin, *Fiz. Tekh. Poluprovodn.* **12**, 273 (1978)

- [Sov. Phys. Semicond. 12, 157 (1978)].
- ¹⁹L. C. Kimerling and J. R. Patel, Appl. Phys. Lett. 34, 73 (1979).
- ²⁰W. Schröter, R. Labusch, and P. Haasen, Phys. Rev. B 15, 4121 (1977).
- ²¹F. Hässermann and H. Schaumburg, Philos. Mag. 27, 745 (1973).
- ²²R. Meingast and H. Alexander, Phys. Status Solidi A 17, 229 (1973).
- ²³A. Gomez, D. J. H. Cockayne, P. E. Hirsch, and V. Vitek, Philos. Mag. 31, 105 (1975).
- ²⁴R. Jones, J. Phys. (Paris) Colloq. C6, 33 (1979).
- ²⁵S. Marklund, Phys. Status Solidi B 92, 83 (1979).
- ²⁶J. M. Andrews, J. Vac. Sci. Technol. 11, 972 (1974).
- ²⁷J. W. Mayer and K. N. Tu, J. Vac. Sci. Technol. 11, 86 (1974).
- ²⁸V. G. Eremenko, V. I. Nikitenko, and E. B. Yakimov, Zh. Eksp. Teor. Fiz. Pis'ma Red. 26, 72 (1977) [JETP Lett. 26, 65 (1977)].
- ²⁹C. Canali, F. Catellani, S. Mantovani, and M. Prudenziati, J. Phys. D 10, 2481 (1977).
- ³⁰R. A. Smith, *Semiconductors* (Cambridge University Press, Cambridge, England, 1964), p. 353.
- ³¹C. T. Sah, L. L. Rosier, and L. Forbes, Appl. Phys. Lett. 15, 161 (1969).
- ³²S. D. Brotherton, Solid State Electron. 19, 341 (1976).
- ³³C. J. Kircher, Solid State Electron. 14, 507 (1971).
- ³⁴A. M. Goodman, J. Appl. Phys. 34, 329 (1963).
- ³⁵S. Mantovani and U. del Pennino, Phys. Status Solidi A 30, 747 (1975).
- ³⁶W. T. Read, Philos. Mag. 45, 775 (1954).
- ³⁷W. Czaia and J. R. Patel, J. Appl. Phys. 36, 1476 (1965).
- ³⁸H. F. Mataré and C. W. Laasko, J. Appl. Phys. 40, 476 (1969).
- ³⁹H. J. Kos and D. Neubert, Phys. Status Solidi A 44, 259 (1977).